STEM CELLS®

REGENERATIVE MEDICINE

Modeling of Photoreceptor Donor-Host Interaction Following Transplantation Reveals a Role for Crx, Müller Glia, and Rho/ROCK Signaling in Neurite Outgrowth

EN L. S. TSAI,[a,b] ARTURO ORTIN-MARTINEZ,[a] AKSHAY GURDITA,[a,b] LACRIMIOARA COMANITA,[a] NICOLE YAN,[a,b] SHEILA SMILEY,[a] VIANNEY DELPLACE,[c] MOLLY S. SHOICHET,[c,d] PHILIP E. B. NICKERSON,[a] VALERIE A. WALLACE[a,b,e]

Key Words. Photoreceptor • Transplantation • Engraftment • Postnatal retina • Donor-host • Neurite • Outgrowth • Crx • Rho/ROCK • In vivo • In vitro

ABSTRACT

The goal of photoreceptor transplantation is to establish functional synaptic connectivity between donor cells and second-order neurons in the host retina. There is, however, limited evidence of donor-host photoreceptor connectivity post-transplant. In this report, we investigated the effect of the host retinal environment on donor photoreceptor neurite outgrowth in vivo and identified a neurite outgrowth-promoting effect of host *Crx*$^{(-/-)}$ retinas following transplantation of purified photoreceptors expressing green fluorescent protein (GFP). To investigate the noncell autonomous factors that influence donor cell neurite outgrowth in vitro, we established a donor-host coculture system using postnatal retinal aggregates. Retinal cell aggregation is sensitive to several factors, including plate coating substrate, cell density, and the presence of Müller glia. Donor photoreceptors exhibit motility in aggregate cultures and can engraft into established aggregate structures. The neurite outgrowth-promoting phenotype observed in *Crx*$^{(-/-)}$ recipients in vivo is recapitulated in donor-host aggregate cocultures, demonstrating the utility of this surrogate in vitro approach. The removal of Müller glia from host aggregates reduced donor cell neurite outgrowth, identifying a role for this cell type in donor-host signaling. Although disruption of chondroitin sulfate proteoglycans in aggregates had no effect on the neurite outgrowth of donor photoreceptors, disruption of Rho/ROCK signaling enhanced outgrowth. Collectively, these data show a novel role of *Crx*, Müller glia, and Rho/ROCK signaling in controlling neurite outgrowth and provide an accessible in vitro model that can be used to screen for factors that regulate donor-host connectivity. STEM CELLS *2019;00:1–13*

SIGNIFICANCE STATEMENT

Poor photoreceptor connectivity in transplants is an unresolved issue. Results of the study show that photoreceptor neurite extension is regulated by Rho/ROCK signaling and report the use of primary retinal cultures as an in vitro platform to investigate donor photoreceptor neurite outgrowth. The results could be used in future work to enhance the connectivity of transplanted photoreceptors.

INTRODUCTION

Inherited photoreceptor retinopathies and age-related macular degeneration are retinal degenerative conditions that are characterized by the loss of light-sensing photoreceptors that initiate vision [1]. Photoreceptors are postmitotic neurons that do not regenerate following loss, and there are no treatments or cures currently available that can restore vision after photoreceptor degeneration. Cell replacement therapy, which involves the transplantation of healthy donor photoreceptor cells adjacent to the surviving retina, is a proposed approach to restore the visual circuit following photoreceptor loss [2]. As the survival of downstream retinal neurons does not depend on the presence of photoreceptors, the potential success of this approach hinges on the concept that surgically transplanted healthy photoreceptors would mature, extend axons, synapse onto their targets, and restore light sensitivity to the retina. Indeed, there is evidence that transplantation of rod and cone photoreceptors results in partial restoration of light sensitivity and visually guided behavior in murine models of retinal

[a]Donald K. Johnson Eye Institute, Krembil Research Institute, University Health Network, Toronto, Ontario, Canada; [b]Department of Laboratory Medicine and Pathobiology, University of Toronto, Toronto, Ontario, Canada; [c]Department of Chemical Engineering & Applied Chemistry, University of Toronto, Toronto, Ontario, Canada; [d]Institute of Biomaterials and Biomedical Engineering, University of Toronto, Toronto, Ontario, Canada; [e]Department of Ophthalmology and Vision Sciences, University of Toronto, Toronto, Ontario, Canada

Correspondence: Valerie A. Wallace, Ph.D., Donald K. Johnson Eye Institute, Krembil Research Institute, University Health Network, 60 Leonard St., Toronto, Ontario, Canada M5T 2S8. Telephone: 416-603-5800; e-mail: valerie.wallace@uhnresearch.ca; or Philip E. B. Nickerson, Ph.D., Donald K. Johnson Eye Institute, Krembil Research Institute, University Health Network, 60 Leonard St., Toronto, Ontario, Canada M5T 2S8. Telephone: 416-603-5800; e-mail: philip.nickerson@uhnresearch.ca

Received October 2, 2018; accepted for publication January 10, 2019; first published online in STEM CELLS *EXPRESS* February 4, 2019.

http://dx.doi.org/10.1002/stem.2985

degeneration [3–7]. This rescue is associated with the presence of GFP-labeled photoreceptors in mice transplanted with GFP-tagged photoreceptor precursor cells, suggesting that donor cells can migrate and synapse with the host retinal neural circuitry. However, more recent evidence indicates that grafted photoreceptors do not integrate into the retina but instead engage in an exchange of cytoplasmic and membrane proteins (material exchange [ME]) [8–12]. In addition to phototransduction proteins, donor-derived GFP was shown to participate in ME prompting a reinterpretation of the extent of donor-host connectivity reported in previous studies. Bona fide synaptic integration of donor photoreceptors with the host retinal circuitry is limited in retinal transplants [13], which is speculated to be because of the absence or abundance of appropriate permissive or inhibitory cues, respectively.

In vivo, photoreceptor connectivity is initiated postnatally and proceeds through several stages beginning with extension of basal axons by postnatal day (P) 0, onset of synapse formation with bipolar and horizontal cells by P2, and refinement of synaptic laminae by P21 [14]. With the exception of Wnt5, which has recently been shown to promote rod photoreceptor axon outgrowth and synaptogenesis with bipolar cells [14], the molecular signals that initiate neurite extension and that guide axons basally toward the inner nuclear layer remain largely unknown. In vitro, rod photoreceptor neurite outgrowth is not enhanced by typical culture substrates [15] but can be promoted by coculture with Müller glia [15] and secreted factors from the retinal pigment epithelium [16]. Unfortunately, the molecular basis for these cellular interactions is unknown, and by extension, the question of how neuritogenesis and connectivity are affected in the context of transplantation currently remains a black box.

To address the issues of impaired connectivity in the context of transplantation, we compared neurite outgrowth of transplanted photoreceptors in wild-type and degenerating murine adult retinas. Although we observed donor cell neurite outgrowth in both contexts, we discovered that this phenomenon was enhanced in degenerating retina recipients. To further characterize the cellular basis for this difference, we developed aggregate cultures from wild-type and *Crx*$^{(-/-)}$ perinatal mouse retinas onto which we seeded donor-age (P4) *Nrl-GFP* rod photoreceptors [17] or *Nrl*$^{(-/-)}$*;Ccdc136*$^{(GFP/GFP)}$ cone-like photoreceptors [18]. Using this approach, we probed the function of several variables including Müller glia, chondroitin sulfate proteoglycans (CSPGs), and Rho/ROCK signaling on photoreceptor neurite outgrowth. Our findings indicate that Müller glia and Rho/ROCK signaling affect outgrowth and that these effects are independent of the neurite-promoting effects of *Crx*$^{(-/-)}$. Collectively, these data demonstrate that ex vivo analysis of donor-host cellular interaction can be used to investigate the regulation of photoreceptor neuritogenesis.

Materials and Methods

Animal and Genotyping

The use of animals in this study was in accordance to the guidelines set out in the Association for Research in Vision and Ophthalmology's statement for use of animals in ophthalmic and vision research. All experiments performed were approved by the University Health Network Research Ethics Board, in accordance with the guidelines of the Canadian Council on Animal Care and in conformity with the University Health Network Care Committee (protocol 3499.10). The following mouse strains were used in this study: C57BL/6J (wild type) (Charles River), *Nrl-GFP* [17], *Nrl*$^{(-/-)}$*;Ccdc136*$^{(GFP/GFP)}$ [18], and *Crx*$^{(-/-)}$ [19, 20] (summarized in Supporting Information Table S1). Genotyping was performed by extracting genomic DNA from ear clips or tail snips using an alkaline lysis buffer (25 mM NaOH [221465, Millipore-Sigma, Oakville, Canada], 0.2 mM EDTA [EDT001.1, BioShop, Burlington, Canada], pH 8.0) for 1 hour at 95°C. The samples were then neutralized with 40 mM Tris-HCl (BP153, Fisher Scientific, Ottawa, Canada), and polymerase chain reaction was performed using gene-specific primer sets (Supporting Information Table S2).

Fluorescence-Activated Cell Sorting Enrichment of Photoreceptors

To enrich for photoreceptors, retinal dissociates from *Nrl-GFP* or *Nrl*$^{(-/-)}$*;Ccdc136*$^{(GFP/GFP)}$ mice were resuspended in 0.5% bovine serum albumin (BSA; A9418, Millipore-Sigma), 25 mM HEPES (HEP001.1, BioShop), 2 mM EDTA, and 0.005% DNase (D5025, Millipore-Sigma) in Ca^{2+}/Mg^{2+}-free phosphate-buffered saline (PBS), and the GFP^+ cells were isolated using fluorescence-activated cell sorting (FACS-Aria IIu, BD Biosciences, Mississauga, Canada) into 10% BSA in Ca^{2+}/Mg^{2+}-free PBS (D8537, Millipore-Sigma) followed by a cell viability assessment using a hemocytometer and 0.4% trypan blue (15250061, Thermo Fisher).

Subretinal Injections and Tissue Processing

Purified photoreceptors were injected into the subretinal space of adult wild-type and *Crx*$^{(-/-)}$ mice as previously described in [9]. Briefly, a blunt 32-gauge needle was inserted tangentially into the subretinal space and 1 µl of cell suspension of 200,000 donor cells was injected. Mice were harvested 21 days postsurgery by exsanguination by PBS and transcardially perfused with 4% paraformaldehyde (PFA; PAR070, Bioshop). For cryosectioning, tissues were fixed for an additional 30 minutes in 4% PFA on ice and then cryoprotected overnight in 30% sucrose (BP-220-1, Fisher Scientific) at 4°C in PBS. After overnight cryoprotection, tissues were equilibrated in 50:50 30% sucrose in PBS:optimal cutting temperature (25608-903, Tissue-Tek, Sakura Finetek, Japan) for 1 hour and subsequently oriented and embedded in plastic molds and sliced at a thickness of 20 µm. Retinal flat mounts were prepared as previously described [21]. Briefly, a suture was placed on the dorsal pole of each eye to maintain the orientation. Retinas were dissected as flattened whole mounts by making four radial cuts (the deepest one in the dorsal pole), postfixed for an additional 30 min in 4% PFA, and kept in PBS until further processing.

Aggregate Culture

To establish retinal aggregate cultures, retinas from wild-type, *Nrl-GFP* or *Crx*$^{(-/-)}$ mice at P1 to P2 were harvested in CO_2-independent media (18045088, Thermo Fisher) and dissociated with papain (Worthington Biochemical, Lakewood, New Jersey) in accordance to manufacturer's directions. The cells were then washed in Ca^{2+}/Mg^{2+}-free PBS and counted using a hemocytometer and 0.4% trypan blue (15250061, Thermo Fisher) viability stain. Dissociated retinal cells were resuspended in retinal explant medium (Supporting Information Tables S3 and S4) and plated at 250,000 cells in 100 µl of media per well of glass-bottomed 96-well plates (P96G-1.5-5-F, Mat-Tek) coated with 70–150 kDa poly-D-lysine

(PDL; P0899, Millipore-Sigma) and laminin (23,017,015, Thermo Fisher). Plates were coated with PDL diluted in sterile water for 3 hours at a concentration of 10 μg/ml at 37°C, followed by three washes with sterile water and coating with laminin diluted in sterile water at a concentration of 1 μg/ml for 1 hour at 37°C, which was removed immediately before plating cells. All cultures were grown in 5% CO_2-buffered incubators at 37°C. After 3 days in vitro (DIV), cultures were refreshed by a 50% media change and cultured for an additional 3 days. For photoreceptor coculture experiments, FACS-enriched GFP$^+$ photoreceptors from P3 to P6 *Nrl*$^{(-/-)}$; *Ccdc136*$^{(GFP/GFP)}$ and *Nrl-GFP* mice were seeded at 25,000 cells per well into established aggregate cultures and cocultured for 3 DIV.

5-Ethynyl-2-deoxyuridine Staining

To label cells in S-phase, cells were cultured in the presence of 5-ethynyl-2-deoxyuridine (EdU; C10338, Thermo Fisher, 10 μM) diluted in retinal explant medium at the start of the culture or 24 hours after plating. EdU was visualized using the Click-iT EdU Alexa-Fluor 555 kit (C10338, Thermo Fisher) in accordance with manufacturer's instructions.

Conditioned Media Experiments

Crx-conditioned media was prepared by removing retinal explant media that had been cultured with *Crx*$^{(-/-)}$ aggregates for 3 DIV. Treatment of established aggregate cultures with *Crx*$^{(-/-)}$-conditioned medium was performed by replacing 50% of the stock media with conditioned media before addition of donor cells.

Experimental Treatment of Aggregate Cultures

Chondroitinase ABC (ChABC; AMS.E1028-2, Amsbio, Cambridge, Massachusetts, 5 U/ml) or the Rho/ROCK inhibitor Y27632 (13624S, Cell Signaling Technologies, Danvers, Massachusetts, 50 μM) was added to the media following the addition of donor cells. To ablate Müller glia in culture, DL-α-aminoadipic acid (AAA; A0637, Millipore-Sigma, 0.4 mM) was added to culture media 4 days prior and washed before the addition of donor cells.

Müller Glia Cell Culture

Mouse Müller glia cells were isolated as previously described [22]. Briefly, 2–4-week-old wild-type retinas were harvested and dissociated with papain (Worthington Biochemical) in accordance to manufacturer's directions. All the dissociated cells were then plated onto 0.1% gelatin (G1890, Millipore-Sigma)-coated 35-mm culture dish (83.3900, Sarstedt, Nümbrecht, Germany) and grown in 5% CO_2-buffered incubators using Dulbecco's modified Eagle's medium (11965092, Thermo Fisher) supplemented with 10% fetal bovine serum (080-150, Wisent, Saint-Jean-Baptiste, Canada) and 1% Pen/Strep (15140122, Thermo Fisher) medium, which was refreshed every 5 days. After two passages, 99% of the remaining cells are Müller glia by immunostaining for glutamine synthetase (GS; data not shown). Müller glia were passaged at least twice to ensure purity before being used in coculture experiments. For coculture experiments, Müller glia were seeded at 50% confluence and cultured for 2–3 days in retinal explant medium before addition of donor photoreceptors and cocultured for an additional 3 days.

Immunocytochemistry

To prepare the aggregate cultures for immunostaining, plates were fixed in 4% PFA for 10 minutes followed by three washes with PBS. Fixed cultures, cryosectioned slides, and flat-mounted retinas were stained in a similar fashion: samples were first blocked in 10% donkey serum (566460, Millipore-Sigma) in 0.5% Triton-X (X100, Millipore-Sigma) PBS for 1 hour at room temperature. Primary antibodies were diluted at the concentrations indicated in Supporting Information Table S5 in 5% donkey serum and 0.25% Triton-X in PBS and were incubated overnight at 4°C. Cultures were then washed three times and incubated with secondary antibodies (summarized in Supporting Information Table S5) in PBS for 1.5 hours at room temperature in a light-protected humidified box. Cell nuclei were counterstained with Hoechst 33342 (62249, Thermo Fisher) diluted in PBS at a concentration 1:15,000 for 20 minutes at room temperature. Cultures were then washed one last time with PBS before being stored in a light-protected container.

Confocal Microscopy, Quantification, and Statistics

Aggregate cultures were imaged using a Zeiss LSM 780 confocal microscope using ×20 and ×40 objective lenses. Acquisition parameters were as follows: resolution was 2048 by 2048 pixels, laser intensity was set at 2%, digital gain at no more than 800, averaging was four, and pinhole size was one airy unit. Comparative images were taken using identical parameters. Live imaging was performed using identical parameters at ×20 magnification and acquired at 15-minute intervals in a CO_2-buffered imaging chamber. Four fields per replicate were sampled for quantification. Both aggregate size and number were quantified using ImageJ (NIH). Aggregates were counted if their lumen stained positive for peanut agglutinin (PNA) in wild-type cultures and/or rhodopsin in purified rod cultures. Neurite quantification was performed on Z-stack images using semiautomatic quantification with the filaments module in Imaris 9.0.2 software (Bitplane, Concord, Massachusetts) (Supporting Information Fig. S1). A two-tailed student's *t* test or a one-way analysis of variance with Scheffe post hoc tests were used to determine significance where appropriate (*$p < .05$, **$p < .01$, and ***$p < .001$) using Microsoft Excel (Microsoft, Redmond, Washington) or Prism 8 (GraphPad, San Diego, California). All data are presented as mean ± SEM.

Results

Donor Photoreceptors Extend Neurites that Are Affected by the Host Retinal Environment

To investigate the morphology of transplanted donor cells both in control recipients and a model of congenital blindness and photoreceptor degeneration, we transplanted P3 to P6 unsorted *Nrl-GFP* cells into the subretinal space of adult wild-type and *Crx*$^{(-/-)}$ [19, 20, 23] retinas, respectively (Fig. 1). *Crx*$^{(-/-)}$ mice were transplanted at 6–8 weeks of age, a stage of progressed but incomplete outer nuclear layer degeneration. Initial screening of donor cells revealed the presence of elaborated, GFP$^+$ cellular processes (Fig. 1A), indicating that heterotopic placement of photoreceptors initiates neuritogenesis from these cells. Evaluation of serial sections revealed a qualitative increase in donor cell neurite formation in *Crx*$^{(-/-)}$ recipients (Fig. 1B). These observations were corroborated when visualized in whole-mount preparations of transplanted retinas imaged using confocal microscopy scans at the apical surface, where the majority of donor cells reside. Specifically, we observed donor cells exhibiting an extensive network of

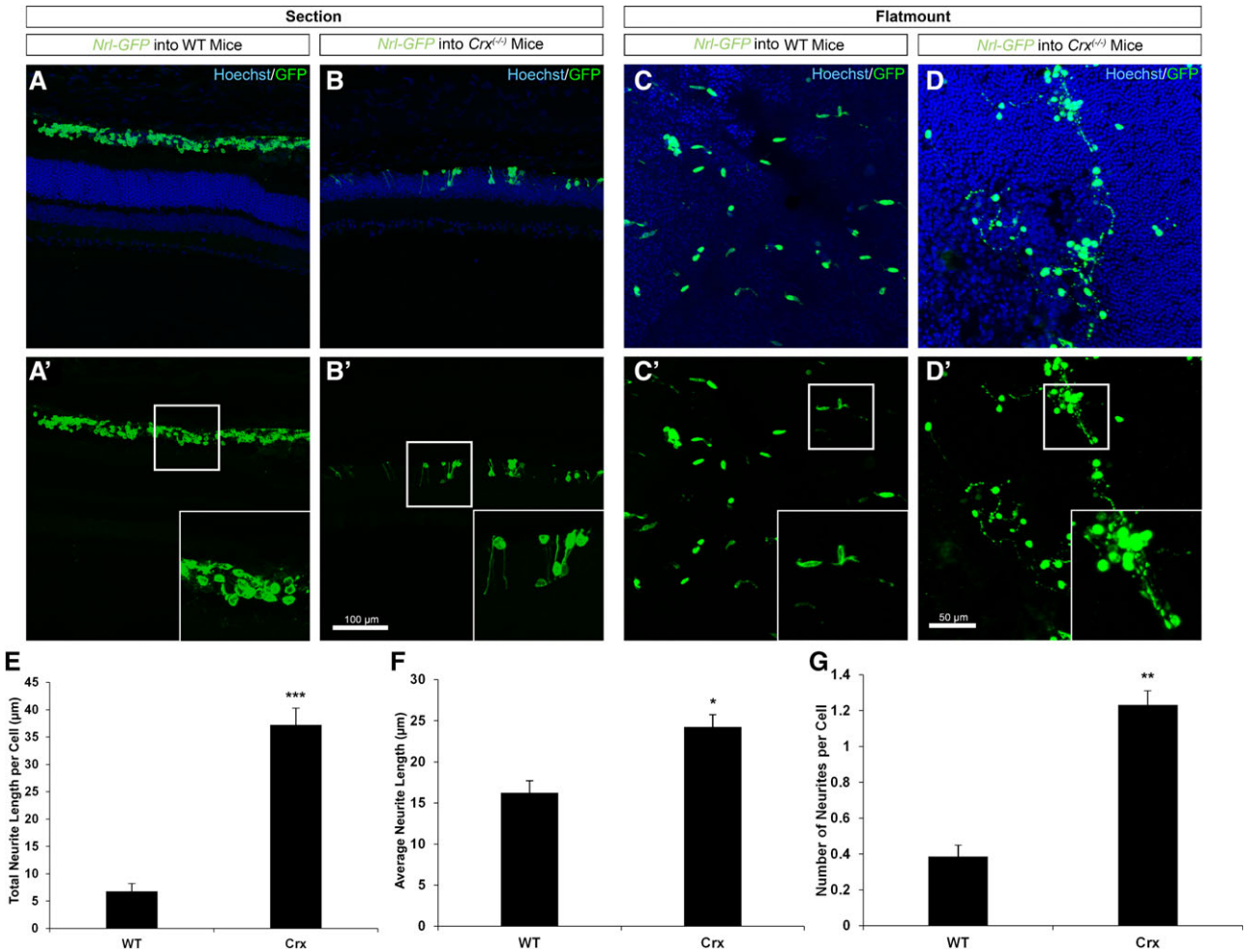

Figure 1. Photoreceptor maturation attenuates neurite extension in vivo. Confocal micrographs of retinal sections **(A–A′, B–B′)** and retinal flat mounts **(C–C′, D–D′)** from $Crx^{(-/-)}$ and WT transplanted eyes. Quantification of *Nrl-GFP* total neurite length per cell **(E)**, average neurite length **(F)**, and number of neurites per cell **(G)** in $Crx^{(-/-)}$ retinas compared with WT (n = 4). *, $p < .05$; **, $p < .01$; ***, $p < .001$. Scale bar in **(A, B)** = 100 µm. Scale bar in **(C, D)** = 50 µm. Abbreviation: WT, wild type.

neurites that extend radially along the apical subretinal surface, which is enhanced in $Crx^{(-/-)}$ compared with wild-type recipients (Fig. 1A, 1D). Three-dimensional reconstruction and analysis of GFP-expressing donors in wild-type and $Crx^{(-/-)}$ retinas revealed an increase in (a) total neurite length per donor cell, (b) average neurite length, and (c) number of neurites per cell in $Crx^{(-/-)}$ recipients (Fig. 1E, 1G). These data indicate that transplanted photoreceptor precursor cells can extend neurites after transplantation, and furthermore, this phenomenon is increased in $Crx^{(-/-)}$ retinas.

Establishment of a Reproducible Aggregate Culture Protocol for Perinatal Mouse Retinal Cells

Many factors could contribute to the enhanced neuritogenesis observed in cells transplanted into the $Crx^{(-/-)}$ eye, including degeneration, injury responses (e.g., gliosis), and altered expression of neurite outgrowth regulators. Although informative, the in vivo transplantation model is exceedingly complex and low throughput, prompting us to develop an aggregate coculture system using donor photoreceptors seeded onto established perinatal retinal cultures (Fig. 2A and Supporting Information Fig. S2). Although not an age-matched proxy to the adult recipient in vivo model, we chose the perinatal time point for aggregate cultures, because it corresponds to a stage when neuritogenesis is maximal and when dissociated retina cells establish some degree of cellular organization by reaggregation [24]. We therefore optimized tissue age, cell density, well size, and coating substrate to generate a reproducible, serum-free aggregate assay for perinatal retinal dissociates on confocal microscope-compatible glass. We determined that the most reproducible cultures were derived from plating P0 to P2 retinal dissociates at 1.28×10^6 cells per centimeter square on PDL/laminin, which supported the aggregation of maximally sized structures by 6 DIV (data not shown). PDL and laminin coating are required, as the former helps aggregates adhere to the culture surface and the latter is essential for aggregate formation. With the exception of retinal ganglion cells, aggregates contained all major retinal lineages in reproducible proportions (Fig. 2B, 2K). Further analysis also showed absence of microglia and endothelial cells in retinal aggregate cultures (Supporting Information Fig. S3). Imaging of the apical rod and cone outer segment markers rhodopsin and PNA, respectively, revealed their localization to the lumen of aggregates, indicating that cells adopt a degree of polarization and maturation under these conditions (Fig. 2B, 2D). To characterize proliferative activity in aggregates, we pulsed cultures with EdU at day 0 and day 1 postplating and quantified the number of EdU^+ cells 24 hours later. We found a significant decrease in the number of EdU^+ cells

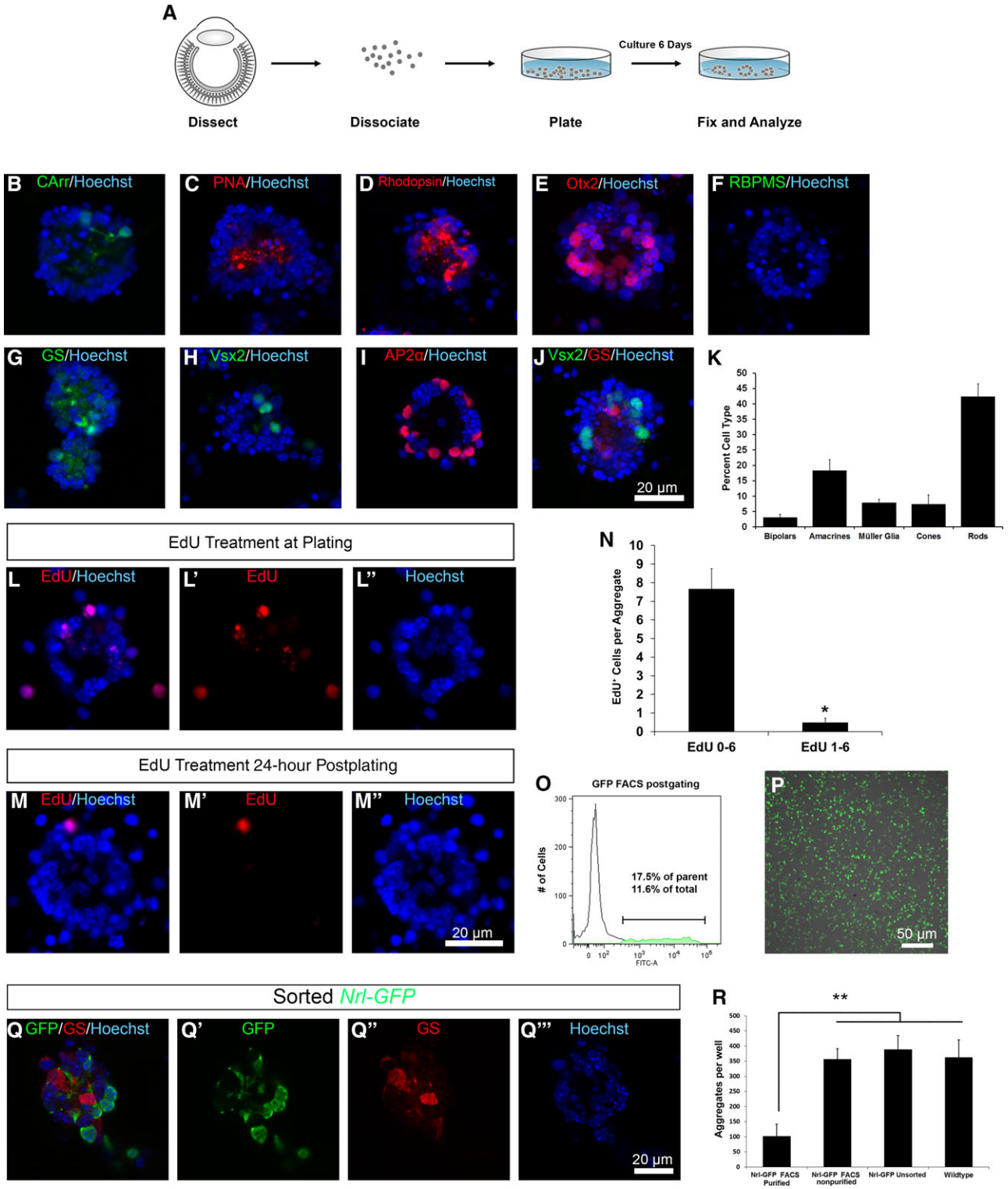

Figure 2. Characterization of donor-host retinal aggregate cultures. **(A):** Schematic showing retinal aggregate protocol. **(B–J):** Immunostaining showing presence of cone and rod photoreceptors, bipolar cells, amacrine cells, and Müller glia and absence of retinal ganglion cells in polarized retinal aggregates. **(K):** Quantification of retinal aggregate composition (N = 24 aggregates, n = 2,845 cells). **(L–L″, M–M″, N):** EdU staining and quantification showing a decrease in S-phase labeling 24 hours postplating (n = 3). **(O):** Flow cytometry of the isolated GFP-expressing photoreceptor population; and **(P)** a low-magnification confocal image of *Nrl-GFP* at the time of plating. Scale bar in **(P)** = 50 μm. **(Q–Q‴):** Immunocytochemistry showing residual Müller glia marker presence in photoreceptor-enriched cultures. **(R):** Quantification showing decrease in aggregate formation in photoreceptor-only cell cultures. *, $p < .05$; **, $p < .01$. Remaining scale bars = 20 μm. Abbreviations: EdU, 5-ethynyl-2-deoxyuridine; FACS, fluorescence-activated cell sorting; GS, glutamine synthetase.

present in individual aggregate structures when the cultures were pulsed 1 day after plating, indicating that the majority of cycling cells detected at day 0 completed their final cell cycle within 24 hours of culture (Fig. 2L, 2N). We then tested whether aggregate formation requires a nonphotoreceptor cell type by comparing the assembly of aggregates derived from either unsorted dissociates or photoreceptors FACS enriched by GFP expression (Fig. 2O, 2P). Aggregate formation was significantly reduced in cultures of FACS-enriched photoreceptors (Fig. 2R), indicating that nonphotoreceptor cells facilitate aggregate assembly. Interestingly, the few aggregates that did form in photoreceptor-only cultures contained Müller glia (Fig. 2Q, 2R), further supporting the interpretation that aggregate formation is dependent on a nonphotoreceptor cell, possibly Müller glia. Although self-organization of retinal cells has been primarily investigated in the context of proliferating cultures [25], the postnatal and postmitotic cultures described here retain the ability to organize with reproducible cell type composition. Furthermore, this cellular organization behavior is associated with the presence of Müller glia.

Purified Photoreceptors Exhibit Motility and Can Integrate into Retinal Aggregates

Recent work from our group and others reports that cells previously thought to arise from donor cell integration following photoreceptor transplantation are a result of transfer of cytoplasmic GFP (ME) from donor to host cells [8–11], reviewed in [26]. We tested whether exogenous GFP-labeled *Nrl-GFP* and *Nrl*$^{(-/-)}$*;Ccdc136*$^{(GFP/GFP)}$ photoreceptors (henceforth referred to as donors) can intercept, physically associate with and transfer GFP to preformed retinal aggregates. Initial screening of donor-host aggregate cocultures revealed many examples of donors that appeared to have integrated into wild-type aggregates (Fig. 3A, 3B′). Previous work has established that the thymidine-analog EdU does not transfer from donor to host photoreceptors (reviewed in [26]), allowing us to determine whether donors truly integrate. We therefore prelabeled donor cells with EdU prenatally and quantified the colocalization of EdU and GFP 3 days after commencement of donor-host aggregate cocultures. EdU^{+}GFP^{+} cells were observed in established aggregates (Fig. 3C, 3D), indicating that they are of donor cell origin. We then independently compared the integration rates of *Nrl-GFP* and *Nrl*$^{(-/-)}$*;Ccdc136*$^{(GFP/GFP)}$ donors by quantifying the proportion of aggregates that contain GFP-expressing cells in each donor condition. *Nrl-GFP* and *Nrl*$^{(-/-)}$*;Ccdc136*$^{(GFP/GFP)}$ donors show differences in their integration rates, as indicated by the percentage of aggregates that contained GFP cells (Fig. 3E, 3F). We used live imaging to conclusively confirm that donor cell integration resulted from donor cell motility rather than aggregates rolling and picking up donor cells (Fig. 3G). Taken together, these data indicate that perinatal *Nrl-GFP* and *Nrl*$^{(-/-)}$*;Ccdc136*$^{(GFP/GFP)}$ photoreceptors can migrate, intercept with, and integrate into postnatal retinal aggregates. This phenomenon occurs at differential rates when comparing *Nrl-GFP* and *Nrl*$^{(-/-)}$*;Ccdc136*$^{(GFP/GFP)}$ photoreceptors, and while we cannot rule out the possibility that photoreceptors can also undergo ME in this context, we show that donor cell integration into aggregates does occur.

Nonphotoreceptor Cell Types Are Necessary for Donor Photoreceptor Neurite Growth

Taking advantage of the sporadic distribution of GFP^{+} photoreceptors in these cocultures allowed us to acquire a detailed evaluation of the morphology of individual donor photoreceptors. We chose to use *Nrl-GFP* instead of *Nrl*$^{(-/-)}$*;Ccdc136*$^{(GFP/GFP)}$ donors, as *Nrl-GFP* donors have a higher GFP intensity, which facilitates morphological analysis. When FACS-enriched *Nrl-GFP* cells are plated on their own at the same density, they fail to elaborate processes, and this effect was independent of coating substrate or cell density (Fig. 4A–4A″). In contrast, we observed that *Nrl-GFP* donors elaborated many GFP-labeled neurite-like processes in cocultures with wild-type aggregates, and this effect was independent of their location within or outside of individual aggregates (Fig. 4B, 4B′″). Analysis of individual donor cells revealed that donor cell neurites stain with the presynaptic marker SV2, indicative of axon-like neurites (Fig. 4C, 4C′″). To rule out the influence of substrate stiffness and rigidity on the inhibition of neurite extension [27], we compared cultures grown on gelatin substrate to those using PDL/laminin. No differences in neurite extension were observed when comparing gelatin to PDL/Laminin (data not shown). Collectively, these data indicate that the initiation of neurite extension by donor cells in this context requires noncell autonomous signaling in the form or the cellular organization provided by the aggregates or a nonphotoreceptor cell type.

The in vivo Crx$^{(-/-)}$ Phenotype Can Be Recapitulated in Donor-Host Aggregate Cocultures

We next sought to identify whether perinatal *Crx*$^{(-/-)}$ retinas can be used to generate aggregate cultures. Retinal dissociates from *Crx*$^{(-/-)}$ mice formed aggregates of similar appearance to wild type (Fig. 5). In vivo, photoreceptors in the *Crx*$^{(-/-)}$ retina are specified but fail to differentiate, upregulate phototransduction pathway proteins and mature morphologically [19]. Similarly, photoreceptors in *Crx*$^{(-/-)}$ aggregates express Otx2, consistent with their specification to the photoreceptor lineage (Fig. 5A–5A″). Unlike wild-type photoreceptors, which normally downregulate *Otx2* as they mature [28], *Crx*$^{(-/-)}$ aggregate cultures maintained Otx2 expression. To determine whether the neurite-promoting effect of the *Crx*$^{(-/-)}$ retina that we observed in vivo is recapitulated in vitro, we generated *Nrl-GFP* donor-*Crx*$^{(-/-)}$ host aggregate cocultures and quantified the formation of GFP^{+} neurites (Fig. 5D, 5D′). *Crx*$^{(-/-)}$ aggregate cocultures exhibited a significant increase in (a) the frequency of donor cells that have neurites, (b) the number of neurites per cell, and (b) total neurite length per cell compared with wild-type cocultures (Fig. 5F, 5H). We next investigated whether the neurite-promoting property of *Crx*$^{(-/-)}$ aggregates was mediated by a secreted factor(s), by treating *Nrl-GFP* donor-wild-type host aggregate cocultures with conditioned medium from *Crx*$^{(-/-)}$ cultures (Fig. 5G) and observed a significant increase in neurite length following addition of *Crx*$^{(-/-)}$-conditioned media. Collectively, these data indicate that aspects of photoreceptor maturation regulated by *Crx* expression influence donor cell neurite outgrowth, in part, through diffusible cues.

Müller Glia Are Essential for Efficient Photoreceptor Neurite Outgrowth in Aggregates

Our evidence that a diffusible cue from *Crx*$^{(-/-)}$ aggregates stimulates photoreceptor neurite outgrowth prompted us to test known cellular sources that may mediate this behavior. Observations from our aggregate system implicate Müller glia as active players in aggregate assembly, and previous work demonstrated a role for these cells in neurite extension in

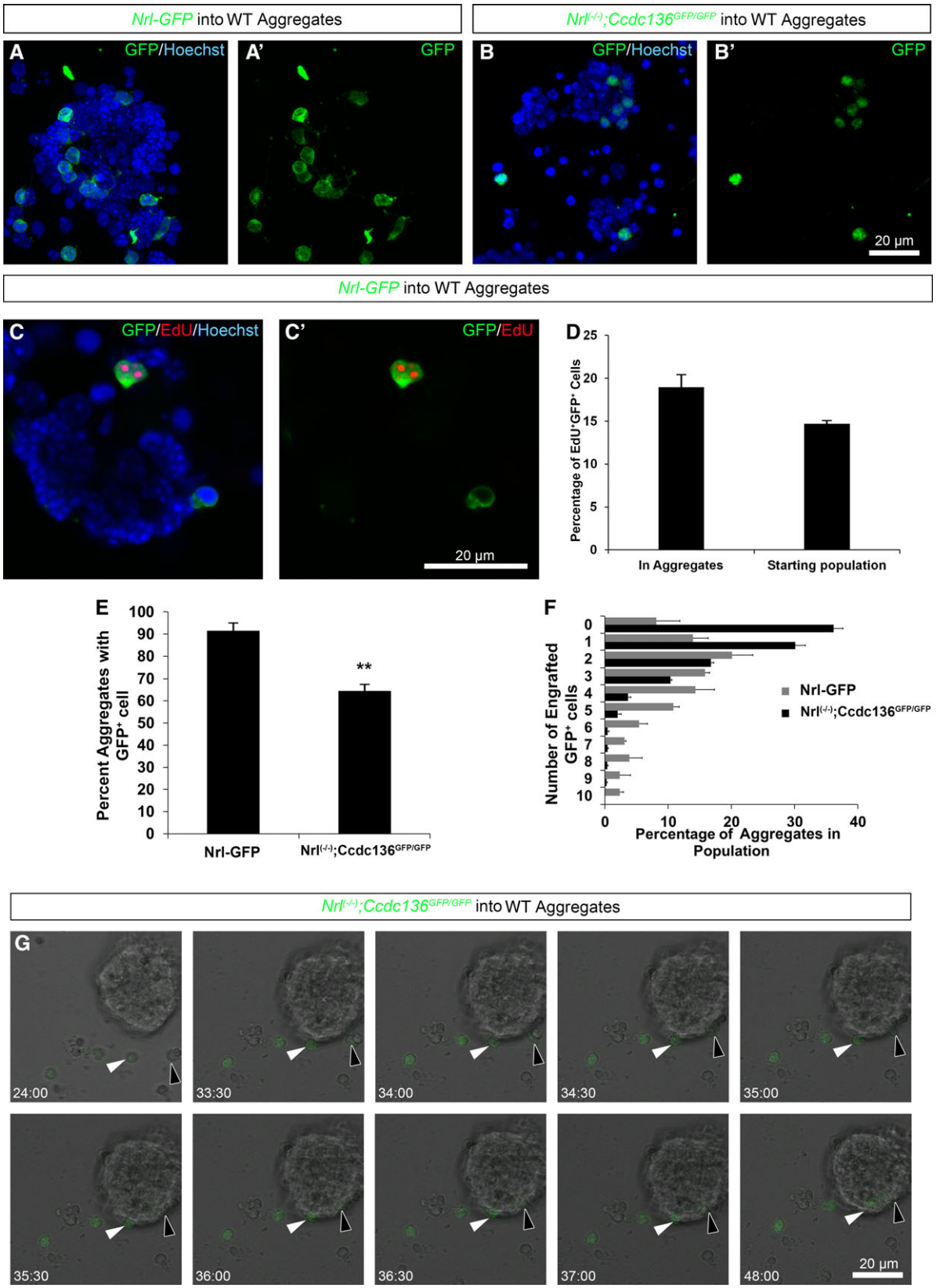

Figure 3. *Nrl-GFP* and *Nrl*$^{(-/-)}$;*Ccdc136*$^{(GFP/GFP)}$ donor photoreceptors engraft at different rates in wild-type aggregates. Examples of GFP-expressing, engrafted *Nrl-GFP* **(A, A′)** or *Nrl*$^{(-/-)}$;*Ccdc136*$^{(GFP/GFP)}$ **(B, B′)** donor cells in wild-type aggregates. **(C, C′):** EdU stain indicating that physically engraftment donors are of donor (in vivo) origin. **(D):** Quantification of EdU indicating the absence of material exchange in these conditions. **(E, F):** Quantification of cell engraftment by donor cell type (N = 9 replicates, n = 1,046 aggregates). **(G):** Time-lapse image showing *Nrl*$^{(-/-)}$;*Ccdc136*$^{(GFPiGFP)}$ donor cell engraftment into wild-type aggregates. **, $p < .01$. Scale bars = 20 μm. Abbreviation: EdU, 5-ethynyl-2-deoxyuridine.

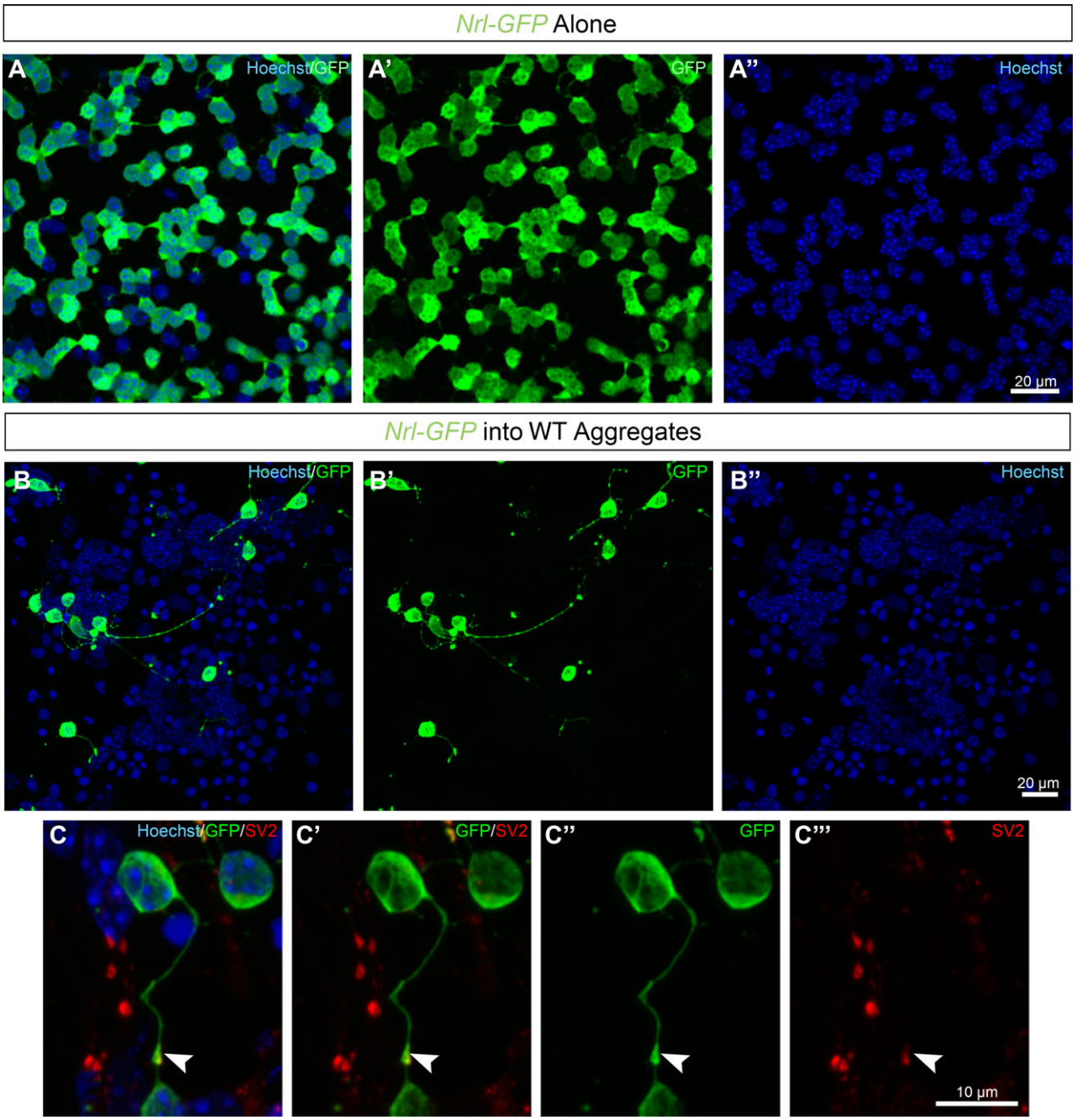

Figure 4. Donor photoreceptors extend neurites in aggregate cultures. **(A–A″):** Purified *Nrl-GFP* photoreceptors fail to elaborate complex neurites when cultured alone under aggregation conditions (n = 6). **(B–B″):** In contrast, *Nrl-GFP* donor cells in aggregate conditions extend long and elaborate neurites (n = 6). Scale bars in **(A–B)** = 20 μm. **(C–C‴):** *Nrl-GFP* neurites stain positive for the synaptic vesicle marker SV2 (arrowhead) (n = 3). Scale bar in **(C)** = 10 μm.

dissociated rat retinal cultures [15]. Aggregates were immunolabeled with GS, glial fibrillary acidic protein (GFAP) and Sox2 to distinguish between Müller glia and retinal astrocytes [29]. The absence of $GFAP^{+}GS^{-}$ (retinal astrocytes) cells and the presence of $Sox2^{+}GFAP^{+}$ and $GS^{+}GFAP^{+}$ colabeled cells (Supporting Information Fig. S3) indicated the presence of Müller glia that were associated with aggregate structures. Colabeling of aggregates with GFAP and *Nrl-GFP* indicated that donor photoreceptor neurite outgrowth does not typically follow the trajectory of Müller glia processes (Fig. 6A, 6B′). To test the requirement for Müller glia on donor cell association with aggregates and neurite outgrowth, we selectively eliminated Müller glia by treating the cultures with the gliotoxin AAA [30–32] 2 days before the addition of donor cells. In both wild-type and $Crx^{(-/-)}$ aggregate cultures (Fig. 6C, 6F′), AAA treatment resulted in a reduction in both total neurite length and average neurite length per *Nrl-GFP* cell (Fig. 6G, 6H). Furthermore, coculturing donor photoreceptors with isolated Müller glia resulted in a marked increase in both the number of neurites per donor cell and total neurite length per cell (Fig. 6I, 6L). These data corroborate previous observations [33] that Müller glia play a role in photoreceptor neuritogenesis.

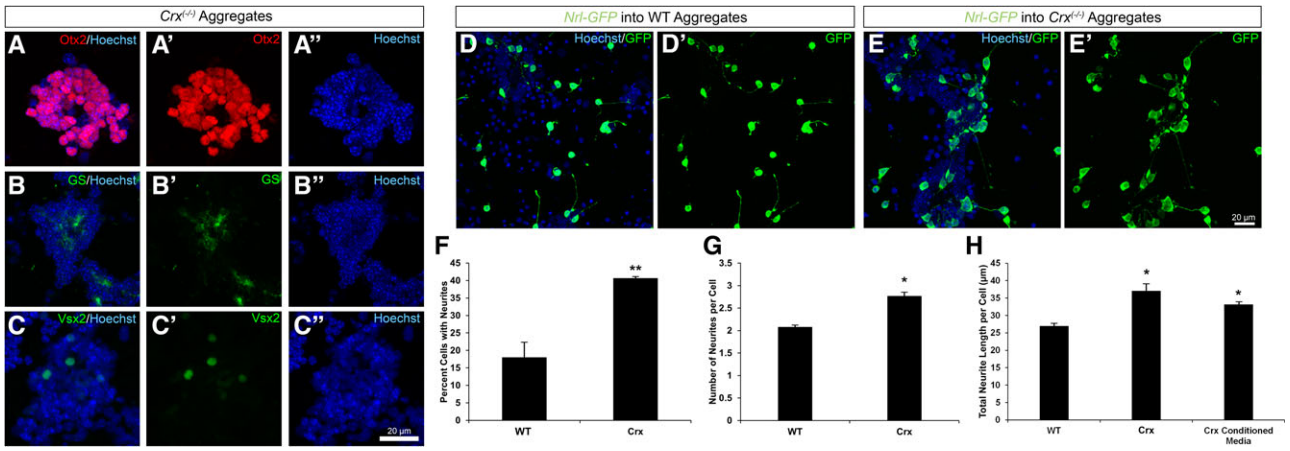

Figure 5. A diffusible factor released from $Crx^{(-i-)}$ aggregates stimulates neurite outgrowth in *Nrl-GFP* donors. **(A–A″, B–B″, C–C″):** Immunostaining showing that $Crx^{(-/-)}$ aggregates maintain Otx2 expression and have similar cell composition to WT aggregates. **(D–D′, E–E′):** Immunostaining showing *Nrl-GFP* donor cells have enhanced neurite extension when cocultured with $Crx^{(-/-)}$ aggregates versus WT aggregates. **(F, G):** Neurite quantification showing an enhancement of cells with neurite and number of neurites per cell (n = 9). **(H):** Quantification showing that $Crx^{(-/-)}$ has enhanced total neurite length per cell and that this effect can be recapitulated by $Crx^{(-/-)}$-conditioned media (n = 9). *, $p < .05$; **, $p < .01$. Scale bars = 20 μm. Abbreviations: GS, glutamine synthetase; WT, wild type.

Photoreceptor Neurite Outgrowth Is Sensitive to Rho/ROCK Signaling

One variable that could account for differences in neurite outgrowth activity observed between wild-type and $Crx^{(-/-)}$ aggregates is the presence of inhibitory cues. Previous work has established that CSPGs, inhibitory substrates for neurite outgrowth [34], are expressed in wild-type mouse outer retinas and are downregulated in multiple models of retinal degeneration [35]. Consistent with these reports, we observed a reduction in CSPG staining in cryosections of adult $Crx^{(-/-)}$ retinas compared with wild-type counterparts (Fig. 7A, 7B). To test the role for CSPGs on donor photoreceptor neurite outgrowth in vitro, we depleted CSPGs in aggregate cultures by treatment with the enzyme ChABC. Neurite outgrowth was unaffected following application of ChABC, suggesting that CSPGs do not play a significant role in photoreceptor neurite outgrowth, at least in this context (Fig. 7E, 7G). Alternatively, many neurite-promoting and growth-inhibiting cues converge on the Rho/ROCK pathway [36], and thus, we asked whether the modulation of this pathway with a ROCK inhibitor (Y27632) would affect photoreceptor neurite outgrowth. Treatment with the ROCK inhibitor significantly increased donor photoreceptor neurite outgrowth in wild-type and $Crx^{(-/-)}$ cocultures (Fig. 7H, 7L). Taken together, these data suggest Rho/ROCK signaling together with Crx-dependent processes contribute to donor cell neurite outgrowth in this coculture model.

Discussion

The mechanisms that regulate photoreceptor connectivity following transplant into the adult retina are poorly understood. Here, we investigated donor photoreceptor competence for neurite extension in vivo and in vitro using cells from the P4 to P6 retina, as this corresponds to the most commonly used stage for mouse photoreceptor precursor transplantation in vivo (reviewed in [37]) and corresponds to the initiation of photoreceptor synaptogenesis in vivo. Establishment of this aggregation culture is both economical and efficient, as primary cells from a single litter of pups can be plated and ready to receive donor cells within 6 days. Although the retinal aggregates described in our assay exhibit less laminar organization than culture preparations of embryonic and induced retinal organoids [38, 39], these perinatal aggregates did form with a high degree of reproducibly. Furthermore, we require minimal starting material to establish our experiments, as an average yield of 1.0×10^7 cells per pup can be used to run 40 experimental replicates in a 96-well plate.

Based on recent findings, few if any donor photoreceptor cell bodies integrate into the host photoreceptor layer post-transplantation [8–12]. We provide evidence that *Nrl-GFP*$^+$ cells can migrate in the cultures and donor cells colabeled with a nuclear marker (EdU) can incorporate into cellular aggregates. Thus, the lack of donor integration in vivo is not because of an inherent inability of photoreceptors to migrate and may instead be related to differences in the environment in terms of age (perinatal in vitro versus adult retina in vivo) [9]. It is unlikely that GFP$^+$ cells monitored for neurite formation represent cells that have acquired GFP from the *Nrl-GFP* cells, because if this was the case, the levels of GFP would be lower as we have observed for host cells with GFP transfer in vivo. We cannot rule out the possibility that ME does take place in our assay; however, it is not convincingly detectable by visual inspection of the cultures and will thus require more sensitive detection methods that are beyond the scope and focus of this study.

We observed that photoreceptor precursors require coculture with retinal aggregates to elaborate long neurite process. This observation is in contrast with the robust neuritogenesis observed in other central nervous system (CNS) neuron cultures, such as transplantable cortical interneurons (reviewed in [40]). Our data are consistent with previous in vitro studies [15] reporting that standard substrates, such as collagen I, laminin, or fibronectin, are insufficient on their own to stimulate photoreceptor neurite outgrowth. The nature of the photoreceptor neurite-promoting activity provided by retinal aggregate in our cocultures is not known, but we suggest that it involves positive cues, as opposed to the suppression of inhibitory cues. We base this reasoning on (a) the observation that culturing photoreceptors at low density, which could dilute inhibitory cues, does not ameliorate neurite outgrowth and (b) reduction of CSPGs, which

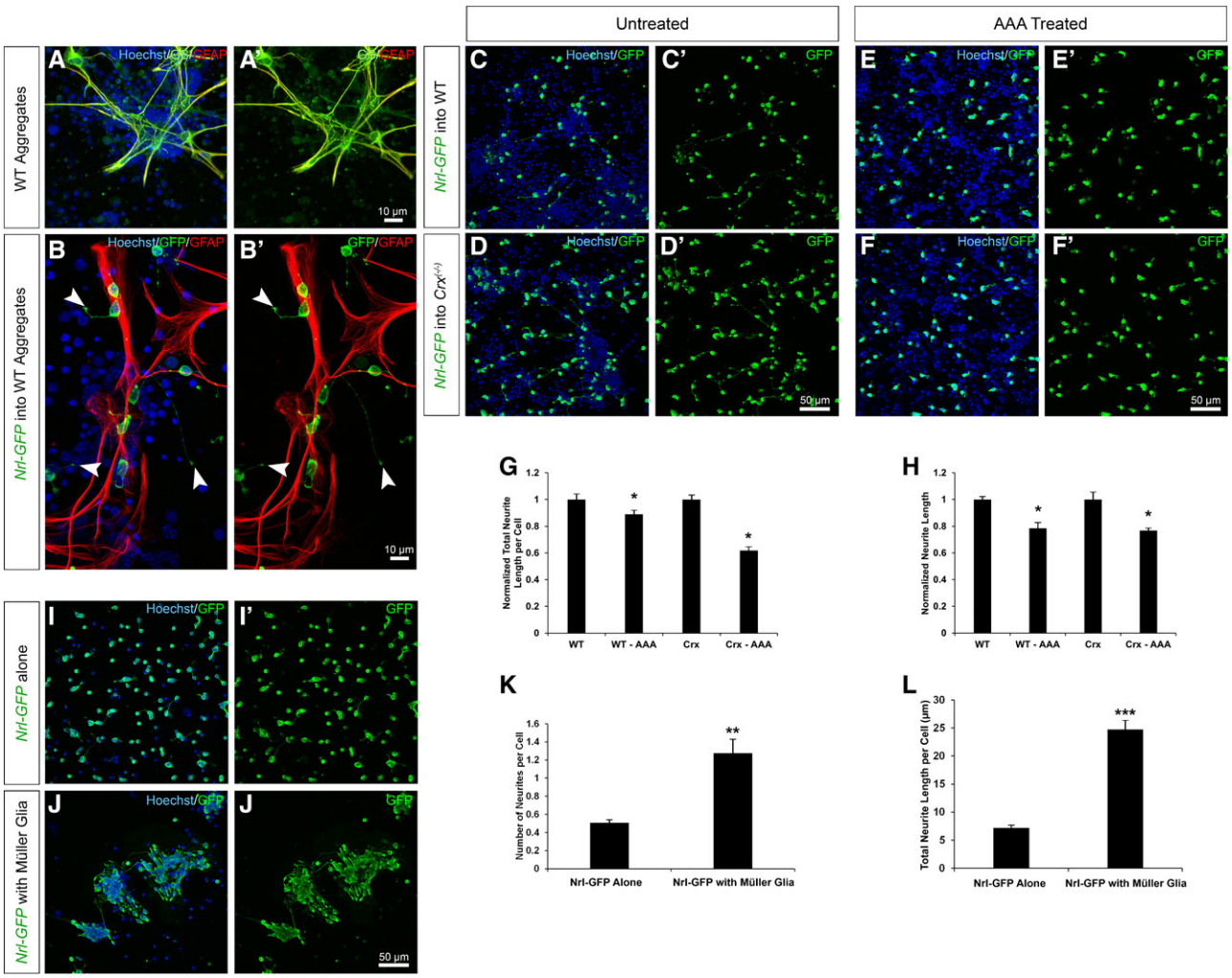

Figure 6. Müller glia are required for donor photoreceptor neurite extension in aggregation cultures. **(A–A′):** The presence of Müller glia in aggregate cultures indicated by coimmunostaining for GFAP and GS. **(B–B′):** *Nrl-GFP* neurites do not grow exclusively along GFAP^{+} Müller glia processes. **(C–C′, D–D′, E–E′, F–F′):** Ablation of Müller glia in both WT and *Crx*$^{(-/-)}$ aggregates following AAA treatment compared with untreated controls. **(G, H):** Quantification showing a decrease in total *Nrl-GFP* neurite length per cell and average neurite length when treated with AAA (n = 3). **(I–I′, J–J′):** *Nrl-GFP* cells alone have limited neurite extension, but *Nrl-GFP* cells cultured with Müller glia extend neurites in a semiorganized fashion. **(K, L):** Quantification of *Nrl-GFP* neurites when cultured alone versus in the presence of enriched Müller glia (n = 3). *, p < .05; **, p < .01; ***, p < .001. Scale bars in **(C–F)** and **(I–J)** = 50 µm. Scale bar in **(A–B)** = 10 µm. Abbreviations: AAA, DL-α-aminoadipic acid; GFAP, glial fibrillary acidic protein; GS, glutamine synthetase.

inhibit axon outgrowth in other contexts (reviewed in [41]), does not significantly affect photoreceptor neurite outgrowth in our cultures. We do show, however, that Rho/ROCK inhibition is sufficient to increase neurite outgrowth in cocultures, suggesting that this phenomenon is regulated by similar pathways observed in other CNS neuron subtypes.

Neurons and glia have mutual interactions that are required for the formation of synaptic connections in the CNS, particularly the callosal neuronal pathfinding [42–44]. Work done in chick and zebrafish models have implicated Müller glia as key players in the laminar organization of retinal cells [45, 46]. Consistent with these observations, our findings also support a role for Müller glia on mouse retinal cell organization in vitro, as the only aggregates that formed in photoreceptor-only cultures contained contaminating Müller glia. Our findings also suggest that Müller glia promote photoreceptor neurite outgrowth, as depleting these cells in the aggregate cultures attenuates donor photoreceptor neurite outgrowth. This observation is consistent with previous studies showing purified Müller glia had significant neurite-promoting effects on rod photoreceptors that appears to be mediated, in part by neural cell adhesion molecules [15]. Curiously, the relationship between photoreceptors in aggregate versus purified Müller glia cocultures is quite different. In cocultures with aggregates, photoreceptor neurites did not appear to be in direct contact or aligned with Müller glia. This is in contrast to photoreceptor-Müller glia cocultures, where photoreceptor neurites grow in very close proximity to Müller glia. The basis for these differences could be severalfold, including culture-associated differences. For example, enriched Müller glia are cultured for several weeks in the presence of serum, whereas the aggregate cultures are serum-free and cultured for up to 1 week. Finally, our findings do not rule out the possibility that other cell types, such as bipolar cells, are also playing a role in neurite outgrowth in our in vitro system.

We observed a striking increase in photoreceptor neurite formation in transplanted *Crx*$^{(-/-)}$ retinas and in donor-host

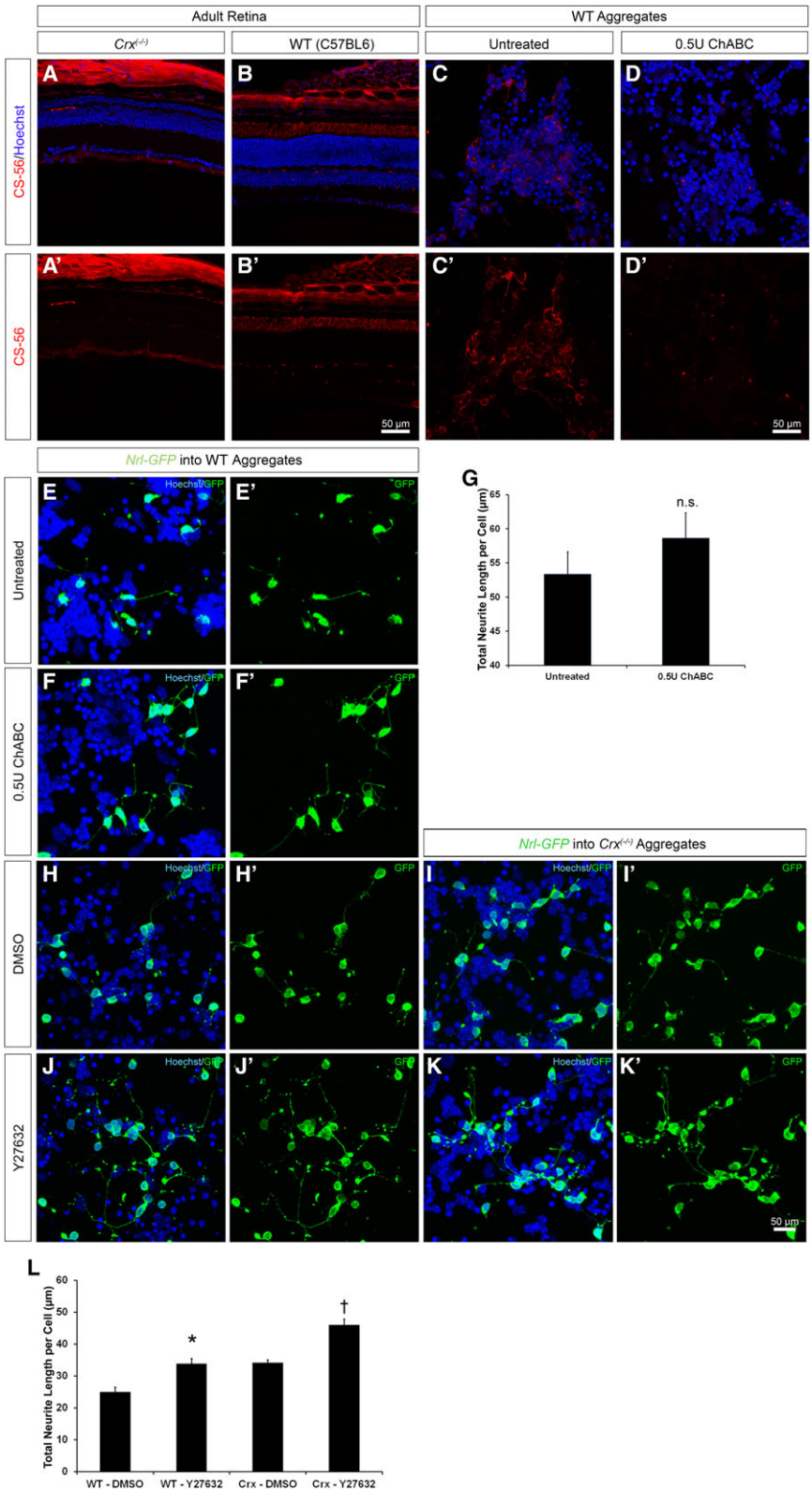

Figure 7. Rho/ROCK inhibition enhances donor cell neurite extension. **(A–A′, B–B′, C–C′, D–D′):** Chondroitin sulfate proteoglycans (CSPG) deposition is reduced in $Crx^{(-/-)}$ retinas compared with WT. **(C–C′, D–D′):** Depletion of CSPG following ChABC treatment of WT donor-host aggregates. Images showing *Nrl-GFP* donor cell neurite extension when cocultured with untreated WT aggregates versus ChABC-treated aggregates **(E–E′, F–F′)**. Quantification showing a slight increase in total neurite length per cell that was not significant (n = 3) **(G)**. Images showing the effects of a Rho/ROCK inhibitor versus DMSO on donor cells cultured with WT and $Crx^{(-/-)}$ aggregates **(H–H′, I–I′, J–J′, K–K′)**. Quantification showing an increase in total neurite length per cell with Rho/ROCK inhibitor treatment in both WT and $Crx^{(-/-)}$ aggregates (n = 3) **(L)**. *, $p < .05$; †, $p < .05$. Scale bars = 50 µm. Abbreviation: ChABC, Chondroitinase ABC; DMSO, dimethyl sulfoxide; n.s., not significant; WT, wild type.

cocultures with $Crx^{(-/-)}$ aggregates. This effect may be mediated in part, by soluble factors, as $Crx^{(-/-)}$-conditioned medium promoted neurite outgrowth. This diffusible cue(s) appears to be independent of Rho/ROCK signaling, as ROCK inhibition further potentiates neurite outgrowth in cultures with $Crx^{(-/-)}$ aggregates. Although the developing and adult $Crx^{(-/-)}$ environments are neurite outgrowth promoting, it is plausible that these effects are mediated by different mechanisms. For example, it is possible that (a) growth-promoting cues persist in the $Crx^{(-/-)}$ eye because of the impairment of photoreceptor maturation or (b) the effect may be caused by the effects of photoreceptor degeneration. Somewhat paradoxically, the neuritogenic phenotype in $Crx^{(-/-)}$ cultures is an interesting contrast to the reported deficiency in synapse formation and connectivity to second-order neurons in the $Crx^{(-/-)}$ retina [47]. The basis for these effects could be related to altered expression of synaptic connectivity factors in the $Crx^{(-/-)}$ environment, which is consistent with transcriptome analysis of $Crx^{(-/-)}$ retinas showing altered expression of at least 18 synapse-related genes [48]. It is possible that the abnormalities in synapse formation may actually promote neuritogenesis if it results in a failure to suppress neurite outgrowth-promoting cues [49]. Consistent with this possibility, aberrant neurite sprouting has been reported in murine retinal degeneration models [50].

Conclusion

Establishment of photoreceptor connectivity is poorly understood. In this current study, we have identified *Crx,* Müller glia, and Rho/ROCK signaling as regulators of photoreceptor neurite outgrowth. Moreover, we have established a novel in vitro platform for studying engraftment, photoreceptor neurogenesis, and axon guidance in the context of photoreceptor transplantation that can be used to uncover mechanisms that mediate this phenomenon.

Acknowledgments

E.L.S.T. is a recipient of Vision Science Research Program studentship. This work was supported by operating grants to V.A.W. from Brain Canada, Foundation Fighting Blindness, Ontario Institute of Regenerative Medicine, Krembil Foundation, and the University of Toronto's Medicine by Design initiative, funded by Canada First Research Excellence Fund.

Author Contributions

E.L.S.T.: conception/design, collection and/or assembly of data, data analysis and interpretation, manuscript writing; A.O.-M., A.G., and N.Y.: conception/design, collection and/or assembly of data, data analysis; L.C.: conception/design, technical support; S.S.: conception/design, collection and/or assembly of data; V.D.: collection and/or assembly of data, data analysis; M.S.S.: conception/design, financial support, data interpretation; P.E.B.N.: data analysis and interpretation, manuscript writing; V.A.W.: conception/design, financial support, data interpretation, manuscript writing, final approval of manuscript.

Disclosure of Potential Conflicts of Interest

The authors indicated no potential conflicts of interest.

References

1 Berger W, Kloeckener-Gruissem B, Neidhardt J. The molecular basis of human retinal and vitreoretinal diseases. Prog Retin Eye Res 2010; 29:335–375.

2 Pearson RA. Advances in repairing the degenerate retina by rod photoreceptor transplantation. Biotechnol Adv 2014;32:485–491.

3 Barnea-Cramer AO, Wang W, Lu SJ et al. Function of human pluripotent stem cell-derived photoreceptor progenitors in blind mice. Sci Rep 2016;6:29784.

4 Lamba DA, Gust J, Reh TA. Transplantation of human embryonic stem cell-derived photoreceptors restores some visual function in Crx-deficient mice. Cell Stem Cell 2009;4: 73–79.

5 MacLaren RE, Pearson RA, Macneil A et al. Retinal repair by transplantation of photoreceptor precursors. Nature 2006;444:203–207.

6 Pearson RA, Barber AC, Rizzi M et al. Restoration of vision after transplantation of photoreceptors. Nature 2012;485:99–103.

7 Santos-Ferreira T, Postel K, Stutzki H et al. Daylight vision repair by cell transplantation. Stem Cells 2015;33:79–90.

8 Decembrini S, Martin C, Sennlaub F et al. Cone genesis tracing by the Chrnb4-EGFP mouse line: Evidences of cellular material fusion after cone precursor transplantation. Mol Ther 2017; 25:634–653.

9 Ortin-Martinez A, Tsai EL, Nickerson PE et al. A reinterpretation of cell transplantation: GFP Transfer from donor to host photoreceptors. Stem Cells 2017;35:932–939.

10 Pearson RA, Gonzalez-Cordero A, West EL et al. Donor and host photoreceptors engage in material transfer following transplantation of post-mitotic photoreceptor precursors. Nat Commun 2016;7:13029.

11 Santos-Ferreira T, Llonch S, Borsch O et al. Retinal transplantation of photoreceptors results in donor-host cytoplasmic exchange. Nat Commun 2016;7:13028.

12 Singh MS, Balmer J, Barnard AR et al. Transplanted photoreceptor precursors transfer proteins to host photoreceptors by a mechanism of cytoplasmic fusion. Nat Commun 2016; 7:13537.

13 Mandai M, Fujii M, Hashiguchi T et al. iPSC-derived retina transplants improve vision in rd1 end-stage retinal-degeneration mice. Stem Cell Rep 2017;8:69–83.

14 Sarin S, Zuniga-Sanchez E, Kurmangaliyev YZ et al. Role for Wnt signaling in retinal neuropil development: Analysis via RNA-Seq and in vivo somatic CRISPR mutagenesis. Neuron 2018;98:109.e8–126.e8.

15 Kljavin IJ, Lagenaur C, Bixby JL et al. Cell adhesion molecules regulating neurite growth from amacrine and rod photoreceptor cells. J Neurosci 1994;14:5035–5049.

16 Gaur VP, Liu Y, Turner JE. RPE conditioned medium stimulates photoreceptor cell survival, neurite outgrowth and differentiation in vitro. Exp Eye Res 1992;54:645–659.

17 Akimoto M, Cheng H, Zhu D et al. Targeting of GFP to newborn rods by Nrl promoter and temporal expression profiling of flow-sorted photoreceptors. PNAS 2006;103: 3890–3895.

18 Smiley S, Nickerson PE, Comanita L et al. Establishment of a cone photoreceptor transplantation platform based on a novel cone-GFP reporter mouse line. Sci Rep 2016;6: 22867.

19 Furukawa T, Morrow EM, Cepko CL. Crx, a novel otx-like homeobox gene, shows photoreceptor-specific expression and regulates photoreceptor differentiation. Cell 1997;91: 531–541.

20 Furukawa T, Morrow EM, Li T et al. Retinopathy and attenuated circadian entrainment in Crx-deficient mice. Nat Genet 1999;23:466–470.

21 Ortín-Martínez A, Nadal-Nicolás FM, Jiménez-López M et al. Number and distribution of mouse retinal cone photoreceptors: Differences between an albino (Swiss) and a pigmented (C57/BL6) strain. PLoS One 2014; 9:e102392.

22 Liu X, Tang L, Liu Y. Mouse Muller cell isolation and culture. Bio Protoc 2017;7:15.

23 Chen S, Wang QL, Nie Z et al. Crx, a novel Otx-like paired-homeodomain protein, binds to and transactivates photoreceptor cell-specific genes. Neuron 1997;19:1017–1030.

24 Kelley MW, Turner JK, Reh TA. Retinoic acid promotes differentiation of photoreceptors in vitro. Development 1994;120:2091–2102.

25 Layer PG, Robitzki A, Rothermel A et al. Of layers and spheres: The reaggregate approach in tissue engineering. Trends Neurosci 2002;25: 131–134.
26 Nickerson PEB, Ortin-Martinez A, Wallace VA. Material exchange in photoreceptor transplantation: Updating our understanding of donor/host communication and the future of cell engraftment science. Front Neural Circuits 2018;12:17.
27 Yeung T, Georges PC, Flanagan LA et al. Effects of substrate stiffness on cell morphology, cytoskeletal structure, and adhesion. Cell Motil Cytoskeleton 2005;60:24–34.
28 Aavani T, Tachibana N, Wallace V et al. Temporal profiling of photoreceptor lineage gene expression during murine retinal development. Gene Expr Patterns 2017;23-24:32–44.
29 Nahirnyj A, Livne-Bar I, Guo X et al. ROS detoxification and proinflammatory cytokines are linked by p38 MAPK signaling in a model of mature astrocyte activation. PLoS One 2013;8:e83049.
30 Brown DR, Kretzschmar HA. The glio-toxic mechanism of alpha-aminoadipic acid on cultured astrocytes. J Neurocytol 1998;27:109–118.
31 Pedersen OO, Karlsen RL. Destruction of Muller cells in the adult rat by intravitreal injection of D,L-alpha-aminoadipic acid. An electron microscopic study. Exp Eye Res 1979; 28:569–575.
32 Rich KA, Figueroa SL, Zhan Y et al. Effects of Muller cell disruption on mouse photoreceptor cell development. Exp Eye Res 1995; 61:235–248.
33 Kljavin IJ, Reh TA. Muller cells are a preferred substrate for in vitro neurite extension by rod photoreceptor cells. J Neurosci 1991; 11:2985–2994.
34 Zuo J, Neubauer D, Dyess K et al. Degradation of chondroitin sulfate proteoglycan enhances the neurite-promoting potential of spinal cord tissue. Exp Neurol 1998;154:654–662.
35 Hippert C, Graca AB, Barber AC et al. Muller glia activation in response to inherited retinal degeneration is highly varied and disease-specific. PLoS One 2015;10:e0120415.
36 Amano M, Nakayama M, Kaibuchi K. Rho-kinase/ROCK: A key regulator of the cytoskeleton and cell polarity. Cytoskeleton 2010; 67:545–554.
37 Jayakody SA, Gonzalez-Cordero A, Ali RR et al. Cellular strategies for retinal repair by photoreceptor replacement. Prog Retin Eye Res 2015;46:31–66.
38 Chen HY, Kaya KD, Dong L et al. Three-dimensional retinal organoids from mouse pluripotent stem cells mimic in vivo development with enhanced stratification and rod photoreceptor differentiation. Mol Vis 2016;22:1077–1094.
39 Nakano T, Ando S, Takata N et al. Self-formation of optic cups and storable stratified neural retina from human ESCs. Cell Stem Cell 2012;10:771–785.
40 Southwell DG, Nicholas CR, Basbaum AI et al. Interneurons from embryonic development to cell-based therapy. Science 2014; 344:1240622.
41 Rauvala H, Paveliev M, Kuja-Panula J et al. Inhibition and enhancement of neural regeneration by chondroitin sulfate proteoglycans. Neural Regen Res 2017;12:687–691.
42 Norris CR, Kalil K. Guidance of callosal axons by radial glia in the developing cerebral cortex. J Neurosci 1991;11:3481–3492.
43 Shu T, Richards LJ. Cortical axon guidance by the glial wedge during the development of the corpus callosum. J Neurosci 2001;21: 2749–2758.
44 Smith KM, Ohkubo Y, Maragnoli ME et al. Midline radial glia translocation and corpus callosum formation require FGF signaling. Nat Neurosci 2006;9:787–797.
45 Eldred MK, Charlton-Perkins M, Muresan L et al. Self-organising aggregates of zebrafish retinal cells for investigating mechanisms of neural lamination. Development 2017;144:1097–1106.
46 Willbold E, Reinicke M, Lance-Jones C et al. Muller glia stabilizes cell columns during retinal development: Lateral cell migration but not neuropil growth is inhibited in mixed chick-quail retinospheroids. Eur J Neurosci 1995; 7:2277–2284.
47 Morrow EM, Furukawa T, Raviola E et al. Synaptogenesis and outer segment formation are perturbed in the neural retina of Crx mutant mice. BMC Neurosci 2005;6:5.
48 Assawachananont J, Kim SY, Kaya KD et al. Cone-rod homeobox CRX controls presynaptic active zone formation in photoreceptors of mammalian retina. Hum Mol Genet 2018;27:3555–3567.
49 Cline HT. Dendritic arbor development and synaptogenesis. Curr Opin Neurobiol 2001;11: 118–126.
50 Strettoi E. A survey of retinal remodeling. Front Cell Neurosci 2015;9:494.


See www.StemCells.com for supporting information available online.